Interactions and Aggregation of Apoferritin Molecules in Solution: Effects of Added Electrolytes

Dimiter N. Petsev,* Bill R. Thomas,*,‡ S.-T. Yau,* and Peter G. Vekilov*,†

*Center for Microgravity and Materials Research and †Department of Chemistry, University of Alabama in Huntsville, Huntsville, Alabama 35899, and ‡Universities Space Research Association, Marshal Space Flight Center, Huntsville, Alabama 35875, USA.

ABSTRACT We have studied the structure of the protein species and the protein–protein interactions in solutions containing two apoferritin molecular forms, monomers and dimers, in the presence of Na^+ and Cd^{2+} ions. We used chromatographic, and static and dynamic light scattering techniques, and atomic force microscopy (AFM). Size-exclusion chromatography was used to isolate these two protein fractions. The sizes and shapes of the monomers and dimers were determined by dynamic light scattering and AFM. Although the monomer is an apparent sphere with a diameter corresponding to previous x-ray crystallography determinations, the dimer shape corresponds to two, bound monomer spheres. Static light scattering was applied to characterize the interactions between solute molecules of monomers and dimers in terms of the second osmotic virial coefficients. The results for the monomers indicate that Na^+ ions cause strong intermolecular repulsion even at concentrations higher than 0.15 M, contrary to the predictions of the commonly applied Derjaguin–Landau–Verwey–Overbeek theory. We argue that the reason for such behavior is hydration force due to the formation of a water shell around the protein molecules with the help of the sodium ions. The addition of even small amounts of Cd^{2+} changes the repulsive interactions to attractive but does not lead to oligomer formation, at least at the protein concentrations used. Thus, the two ions provide examples of strong specificity of their interactions with the protein molecules. In solutions of the apoferritin dimer, the molecules attract even in the presence of Na^+ only, indicating a change in the surface of the apoferritin molecule. In view of the strong repulsion between the monomers, this indicates that the dimers and higher oligomers form only after partial denaturation of some of the apoferritin monomers. These observations suggest that aggregation and self-assembly of protein molecules or molecular subunits may be driven by forces other than those responsible for crystallization and other phase transitions in the protein solution.

INTRODUCTION

An important aspect of the solution behavior of proteins is that of their stability against formation of oligomers (dimers, trimers, etc.). This stability is determined by the interactions between the protein molecules. Furthermore, the biological functions of the proteins, such as enzyme–ligand binding, metabolic interactions, etc., are strongly affected by their immediate environment in the solution that may contain structured water, hydrated cations or anions, organic molecules, polymers, and amphiphilic molecules. The interactions between same molecules are a sensitive probe of this immediate solution environment. Data about the interactions are also needed for control over the crystallization pathways. Protein crystallization is a necessary step in the studies of the molecular structure by diffraction methods, and recent evidence suggests that there is a direct correlation between the pair interactions and crystallization behavior of proteins (George and Wilson, 1994; Rosenbaum and Zukoski, 1996; Velev et al., 1998). Another aspect of crystallization is related to protein aggregation. Should the proteins in a solution aggregate, the formed oligomers are often the main impurity (Thomas et al., 1998) that has undesired effects on the crystallization processes, the quality of the grown crystals, and hence on their suitability for x-ray structure determinations (Vekilov et al., submitted for publication).

Investigations of protein solution behavior have relied on the strong similarities of protein's molecular size and properties to those of colloidal dispersions. Within this approach, the macroscopic properties (osmotic pressure, light scattering), solution dynamics (diffusion) and stability of protein solutions have been described within the framework of the methods and approaches relevant to colloid science (Derjaguin et al., 1987; Verwey and Overbeek, 1948), usually referred to as Derjaguin–Landau–Verwey–Overbeek (DLVO) theory.

Convenient methods to study the interactions and aggregation of polymer solutions and colloidal dispersions are based on light scattering [e.g., Schmitz, 1990]. Static light scattering (SLS) measures the time-averaged intensity of the scattered light and relates it to the osmotic compressibility and the second virial coefficient of the interacting particles. Dynamic light scattering (DLS), on the other hand, measures the time auto-correlation function of the scattered light, which yields the solute diffusion coefficient. The diffusion coefficient is related to the size of the dissolved molecules, in terms of hydrodynamic diameter, and thus provides important complementary information, inaccessible to SLS only. The diffusivity also depends on the thermodynamic interactions (second osmotic virial coefficient),

Received for publication 27 September 1999 and in final form 7 January 2000.

Address reprint requests to Peter G. Vekilov, Center for Microgravity and Materials Research Department of Chemistry, University of Alabama in Huntsville, Huntsville, AL 35899. Tel.: 256-890-6050; Fax: 256-890-6944; E-mail: peter@cmmr.uah.edu.

0006-3495/00/04/2060/10 $2.00

but this dependence is shadowed by the hydrodynamic interactions between the particles. Thus, DLS is a less sensitive probe of the pair molecular energy than SLS.

In this paper, we study solutions of apoferritin, the hollow shell of the iron-storage protein ferritin. Apoferritin readily forms crystals in sodium acetate buffer containing certain amounts of $CdSO_4$ (Thomas et al., 1998). Using samples, pretreated by size-exclusion chromatography, we investigate the solution properties of monomers (single apoferritin molecules) and molecular dimers in the presence of Na^+ and Cd^{2+} ions. The size of the monomers and dimers is determined using DLS, and, independently, by atomic force microscopy carried out in situ, during crystallization of the protein. The results on the dimers' shape and interactions suggest that the protein aggregation and self-assembly pathways may differ from those leading to crystal formation.

The results for the monomer interactions suggest strong repulsion of non-DLVO type at high solution ionic strength. We speculate that this is due to hydration forces. These forces have generally been attributed to water structuring in the vicinity of the interacting surfaces (Marcelja and Radic, 1976; Besseling, 1997; Forsman et al., 1997). Other explanations are based on entropic repulsion associated with the constrained thermal mobility of the surface groups (Israelachvili and Wennerstrom, 1996), excluded volume of the hydrated counterions (Israelachvili, 1991; Pashley, 1981a,b, 1982; Pashley and Israelachvili, 1984), or local variation of the dielectric constant (Basu and Sharma, 1994; Henderson and Lozada-Cassou, 1986, 1994). More elaborate theories, considering combinations of some of the above factors, were also developed (Paunov et al., 1996; Paunov and Binks, 1999; Trokhymchuk et al., 1999). Recent studies of the coagulation kinetics of protein-stabilized colloidal particles implicate hydration repulsion as a factor for increased stability at high ionic strength (Molina-Bolivar et al., 1996, 1997, 1998; Molina-Bolivar, 1999; Molina-Bolivar and Ortega-Vinuesa, 1999). Thus, despite the theoretical ambiguity surrounding hydration forces, they are often encountered in experiments.

Finally, we present results on the influence of $CdSO_4$ on the molecular interactions and show that even small amounts of Cd^{2+} ions suffice to convert significant repulsion into attractive interaction.

MATERIALS

The apoferritin and electrolytes used in the experiments were obtained from Sigma Chemical Co. (St. Louis, MO). It was dissolved in sodium acetate buffer (NaAc) at pH = 5.0. The buffer was prepared by dissolving sodium acetate in water and subsequent titration with acetic acid. Hence, the concentration of $NaOOCCH_3$ (NaAc) equals $[Na^+]$. A MilliRO/Q grade water (Millipore, Bedford, MA) was used for all solution preparations. In some cases, $CdSO_4$ was added to the sample.

METHODS

Fast protein liquid chromatography

The commercial apoferritin solutions were characterized using size-exclusion fast protein liquid chromatography (FPLC). A Pharmacia Biotech (Uppsala, Sweden) Superose 6 HR 10/30 column was used. The mobile phase was 0.2 M NaAc solution flowing at 0.5 ml/min rate. In addition to the UV detector of the FPLC device, a Mini-Dawn light scattering detector (Wyatt Technologies, Santa Barbara, CA) was included. The combination of the two detectors allows identification of low amounts of the high molecular-weight components, and direct determinations of the molecular masses of the eluding fractions.

The signal traces from the two detectors of a typical FPLC separation of commercial apoferritin are shown in Fig. 1. Using this method, we separated the fractions of monomers, dimers, trimers, and higher oligomers. Gel electrophoresis analyses of the various fractions indicate that the fractions labeled Monomer and Dimer contain single species. Both methods show that the molecular masses of the fractions are, respectively, equal or double that of apoferritin. The fraction labeled "Trimer" is a mixture of oligomers containing species with molecular mass about three times that of apoferritin. Details of the analysis and separation are given in Thomas et al. (1996).

Dynamic light scattering

The dynamic light scattering measurements were performed on a Brookhaven 200 SM goniometer with HeNe laser (Spectra Physics 127/V, 35 mV, Mountain View, CA), operating at 632.8 nm wavelength. The method is based on the collected auto-correlation function of the scattered field amplitude E_S (Pusey and Tough, 1985; Schmitz, 1990)

$$g^{(1)}(\tau) = \frac{\langle E_S(t)E_S^*(t+\tau)\rangle}{\langle |E_S|^2\rangle}. \quad (1)$$

For relatively monodisperse samples, a cumulant expansion of the auto-correlation function can be applied

$$\ln g^{(1)}(\tau) = \sum_n K_n \frac{(-\tau)^n}{n!}, \quad (2)$$

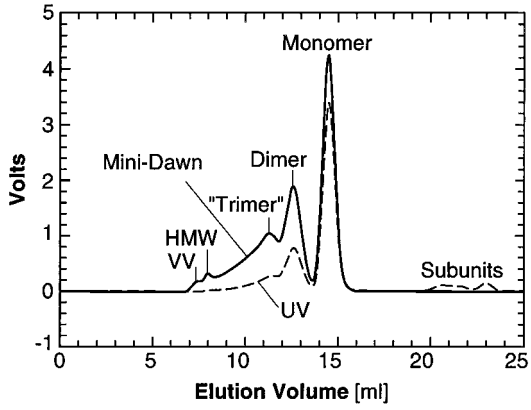

FIGURE 1 Size-exclusion FPLC analysis of commercial apoferritin solution using UV and Mini-Dawn detection at the column exit. HMW and VV, high molecular weight and void-volume components, respectively (Thomas et al. 1998).

where the coefficients K_n can be calculated as

$$K_n = (-1)^n \lim_{\tau \to 0} \frac{d^n}{d\tau^n} \ln g^{(1)}(\tau). \quad (3)$$

Then, the diffusion coefficient of the molecules is then given by

$$D = \frac{K_1}{q^2}, \quad (4)$$

where, with λ is the used wavelength, n is the solution refractive index, and θ is the angle of data collection measured from the direction of the beam passing through the sample,

$$q = \frac{4\pi n}{\lambda} \sin\left(\frac{\theta}{2}\right). \quad (5)$$

The diffusion coefficient, determined from Eq. 4 can be related to the molecular size using the Stokes–Einstein expression (Pusey and Tough, 1985; Schmitz, 1990),

$$D = \frac{kT}{3\pi\eta d_h}, \quad (6)$$

where d_h is the hydrodynamic diameter of the molecule, η is the solvent viscosity and kT is the thermal energy.

If the cumulant method is inapplicable, e.g., for broad, irregularly shaped distributions, or if multiple peaks in the distribution are found, more sophisticated methods have to be used. The most popular method for treatment of such systems is called CONTIN (Provencher, 1979, 1982a,b). For monodisperse samples, both methods yield close values.

Eq. 6 relates the diameter of spherical particle to their experimentally measurable diffusivity. Yet, data about the geometric parameters of nonspherical particles can still be extracted from diffusivity determinations if one makes an assumption about their shape. Thus, for a prolate spheroid, i.e., the envelope around two touching spheres, we could use the hydrodynamic mobility expressions derived by Brenner (1974). This yields for the parallel and perpendicular friction modes, respectively,

$$f_\parallel = \frac{8\pi\eta L}{r^2(2\beta + \alpha_\parallel)}, \quad (7)$$

$$f_\perp = \frac{8\pi\eta L}{2r^2\beta + \alpha_\perp}, \quad (8)$$

where L is the length of the spheroid and $r = L/d$, d is its diameter, and

$$\alpha_\parallel = \frac{2(r^2\beta - 1)}{(r^2 - 1)}, \qquad \alpha_\parallel = \frac{r^2(1 - \beta)}{(r^2 - 1)}, \quad (9)$$

with

$$\beta = \frac{\cosh^{-1}(r)}{r(r^2 - 1)^{1/2}}.$$

Because

$$D_\perp = \frac{kT}{f_\perp} \quad \text{and} \quad D_\parallel = \frac{kT}{f_\parallel}, \quad (10)$$

the effective diffusion coefficient could be written as

$$D = \tfrac{1}{3}(2D_\perp + D_\parallel). \quad (11)$$

By equating the measured diffusion coefficient, Eq. 4, to the right-hand side of Eq. 11, one gets an equation relating a measured quantity to the geometrical parameters of the spheroid. Then, d_h in Eq. 6 has the meaning of effective size.

Static light scattering

The static light scattering experiments were performed on the same equipment as was DLS. The refractive index increment (dn/dC_p) necessary to interpret those data was measured using an Optilab (Wyatt Technologies, Santa Barbara, CA) device, operating at the same wavelength as the laser used for light scattering. Static light scattering is based on determinations of the concentration dependence of the scattered light intensity. The results are then plotted as (Zimm, 1948)

$$\frac{KC_p}{R_\theta} = \frac{1}{M_w}(1 + 2A_2M_wC_p), \quad (12)$$

where M_w is the molecular mass of the protein, C_p is the protein concentration in g/ml, R_θ is the Rayleigh ratio, and K is an optical constant calculated from

$$K = \frac{1}{N_A}\left(\frac{2\pi n_0}{\lambda^2}\right)^2\left(\frac{dn}{dC_p}\right)^2. \quad (13)$$

In Eq. 13, N_A is Avogadro's number, λ the wavelength, n_0 the refractive index of the solution sans protein, and dn/dC_p is the refractive index increment with protein concentration. The quantity A_2 in Eq. 12 is the second osmotic virial coefficient in ml M/g^2 units. If the protein concentration is expressed in volume fraction units, the virial coefficient adopts a convenient dimensionless form

$$B_2 = 12\int_0^\infty \left\{1 - \exp\left[-\frac{U(r)}{kT}\right]\right\} r^2\, dr. \quad (14)$$

For the particular case of hard sphere-type interaction $U(r)$ (note that this is not $U(r) = 0$), $B_2 = 4$ (McQuarrie, 1973) and is due to the finite size of the molecules. Thus, values of the second osmotic virial coefficient lower than four indicate an overall attractive interaction energy between finite-size particles. At the same time, values greater than 4 evidence stronger (than the one due to finite size) repulsion. The most common reason for such repulsion, in the case of colloids, is electrostatics, but other interactions could also be responsible.

It is convenient to rewrite Eq. 12 in the form,

$$\frac{KC_pM_w}{R_\theta} = 1 + 2B_2\phi, \quad (15)$$

where ϕ is the protein volume fraction. Comparing Eqs. 12 and 15, we get an expression relating the dimensional viral coefficient, A_2, to the dimensionless B_2:

$$B_2 = \frac{6A_2M_w^2}{\pi N_A d_h^3}. \quad (16)$$

Atomic force microscopy

Adsorption of the dimer at the crystal face and its incorporation into the crystals were studied by atomic force microscopy (AFM) using a Nanoscope IIIa from Digital Instruments (Santa Barbara, CA). Crystallization took place from a 1-mg/ml solution on a glass substrate at room temperature stabilized to 23.0 ± 0.3°C. The equilibrium solution concentrations

C_e = 23 μg/ml was determined as C at which steps (i.e., the edges of the uncompleted crystal layers) stopped advancing, before dissolution retreat at $C < C_e$. AFM images of the growing crystal surface were collected in situ in the AFM fluid cell during the growth of the crystals using the tapping imaging mode of the device. When chromatographically purified material is used, apoferritin crystals are faceted by (111) faces with a typical beehive arrangement of the molecules. The crystals grow by the spreading of layers generated by surface nucleation. The layer thickness is 10.5 nm, and the distance between the centers of the quasi-spherical ferritin monomers is 13 nm, in agreement with the respective crystallographic values: 10.6 and 13.0 nm.

RESULTS AND DISCUSSION

The structure of apoferritin monomers and dimers

The dynamic light scattering results for apoferritin monomer, dimer, and trimer fractions are presented in Fig. 2 and Table 1. The size-distributions shown in Fig. 2 are obtained using the CONTIN algorithm (Provencher, 1979; 1982a,b). No concentration dependence of the measured diffusion coefficient was observed for the range of protein and salt concentrations we used. We see that all three fractions are relatively monodisperse. The variance of the distribution is 0.167 for the monomers and 0.119 and 0.140 for dimers and trimers, respectively. Accordingly, the average hydrodynamic radii in Table 1 obtained by CONTIN and the cumulant expansion methods are close. The difference in the sizes resulting from the two methods is ~10% for the monomers and even less for dimers and trimers. The sizes of the monomers are also in agreement with data available in the literature (Hempstead et al., 1997), which claim that the apoferritin diameter is about 12 nm.

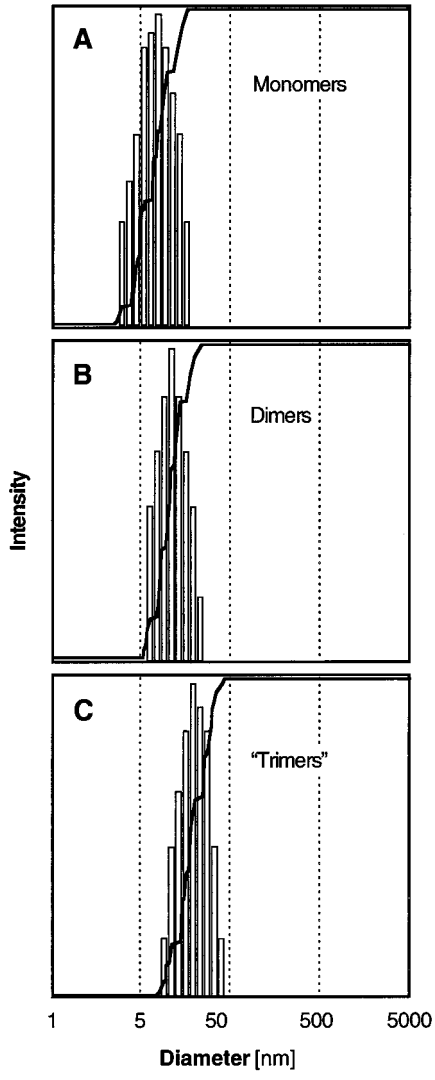

FIGURE 2 CONTIN results for the size distribution of the apoferritin fractions after separation by FPLC.

Direct comparisons of the sizes with published data are not possible for the dimer and trimer because the DLS yields an effective size (diameter) that can be directly correlated to the geometry of the molecule only for spherical objects. When two monomers collide to form a dimer, they can either stick without destroying their separate spherical shapes, or coalesce into a single sphere with a double volume as illustrated in Fig. 3. The second option would require a substantial change in the arrangement of the molecular subunits.

For both cases, based on the diffusion coefficient for the monomer, we can estimate the expected diffusion coefficient of the dimer. For the first case, we assume an anisotropic molecular shape (prolate spheroid) with diameter, d, equal to that of a single molecule, and length, L, equal to two monomer diameters (Fig. 2 *B*). Using Eqs. 6–11, we get $D = 2.30 \times 10^{-7}$ cm^2/s. For the case of coalescing molecules, we use Eq. 6 with diameter

$$d_{\text{eff}} = d\sqrt[3]{2} \tag{17}$$

and get $D = 2.54 \times 10^{-7}$ cm^2/s. The two diffusivities are close, but a comparison with the two values in Table 1 resulting from cumulant and CONTIN analyses of the experimental data, indicates that the anisotropic option is more likely.

For a direct test of the above conclusion as to the shape of the dimer, we viewed the surface of growing apoferritin crystals with AFM (Yau and Vekilov, manuscript in preparation). The observations reveal clusters adsorbed on the

TABLE 1 Diffusion coefficients, D, and hydrodynamic diameters, d_h, for the apoferritin fractions: monomers, dimers, and trimers in the absence of $CdSO_4$.

Aggregate Type	$D_{\text{eff}} \times 10^7$, cm^2/s (second cumulant)	$D_{\text{eff}} \times 10^7$, cm^2/s (CONTIN)	d_h, nm (second cumulant)	d_h, nm (CONTIN)
Monomers	3.19	3.57	12.70	11.40
Dimers	2.21	2.37	18.40	17.10
"Trimers"	1.48	1.43	26.75	30.00

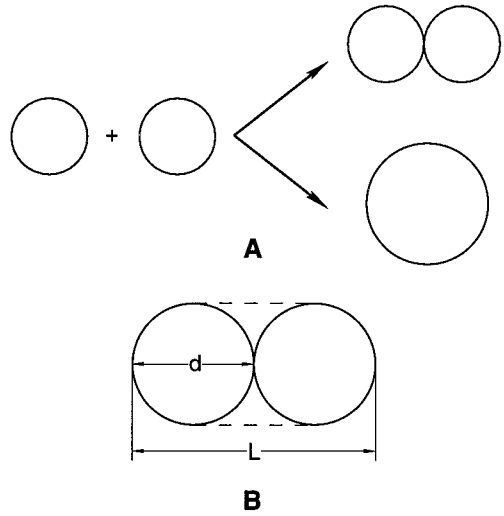

FIGURE 3 (*A*) Two options for apoferritin dimerization. (*B*) Structure and parameters of two stuck apoferritin molecules.

terraces between the growth steps, such as the one in Fig. 4 *A*. The image of a cluster is a convolution of the cluster shape and its molecular vibrations, with effects due to multiple AFM tips. Monitoring a step that approaches and incorporates the cluster in Fig. 4, *B–D* removed these obscuring effects: Fig. 4, *B* and *C* show that the clusters are apoferritin dimers shaped as two bound monomer spheres. The dimers occupy three, rather than two, monomer lattice sites, which suggests that the arrangement of the two monomers in the dimer may be different from that between two monomers in the lattice (Vekilov et al., submitted for publication).

Note that the dimers were not generated by addition of Cd^{2+} ions to the solution to induce crystal formation. They are present in the initial solution before the chromatography separation. Hence, these aggregates are not a preliminary step in apoferritin crystal nucleation or growth. This conclusion is supported by the AFM observation of monomers attaching to the growth sites at the crystal surface and thus becoming part of the crystal (Yau and Vekilov, manuscript in preparation). On the contrary, dimers, trimers, etc. act as impurities and their presence is known to compromise the crystallization process (Thomas et al., 1998). A legitimate question is what are the reasons for such noncrystallographic aggregation, especially in view of the overall repulsive interactions between apoferritin monomers in the presence of NaAc? We speculate that only apoferritin monomers that have undergone a partial denaturation (e.g., slight rearrangement of the 24 subunits, or opening of the loop regions in the peptide chain to reveal the hydrophobic regions of the helices) can partake into the formation of dimers, trimers, and higher-order aggregates. This denaturation obviously does not significantly change the shape and size of the individual monomers, but exposes groups that locally decrease the repulsion and increase the attraction between them. Because such nonspecific forces constitute the bonds within the dimers, it is understandable why they never incorporate in the apoferritin crystal lattice as an integral component, but always cause defects (Thomas et al., 1998; Vekilov et al., submitted for publication; Yau and Vekilov, manuscript in preparation).

If our speculation about the partial denaturation is correct, we would expect it to affect not only the formation of the dimer, but also the dimer–dimer interactions in the solution. Indeed, see below, dimers exhibit attraction under conditions where the monomers strongly repel. Furthermore, the exposed attractive contact sites should affect the interaction of the dimers with a monomer crystal surface and cause the preferential adsorption of the dimers on the crystal surface. Again, AFM observations similar to those in Fig. 4, which

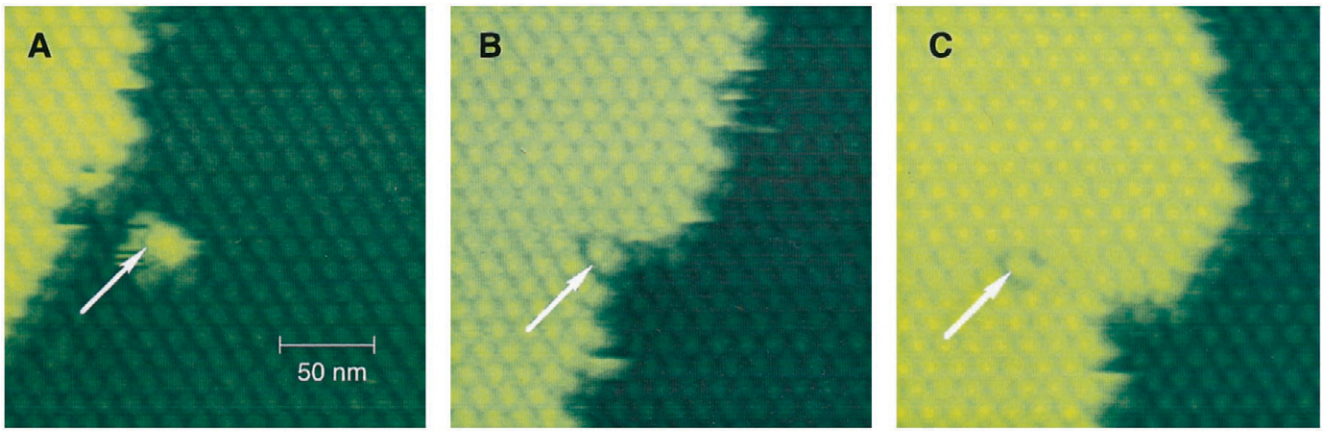

FIGURE 4 In-situ AFM images of the growing crystal surface. (*A*) Growth steps with adsorbed impurity clusters and related point defects on the terraces between the steps. (*B–D*) Incorporation of a cluster, indicated by arrows by a step. *C* and *D* Deconvolution of cluster shape from vibration and multiple tips effects allows identification as a ferritin dimer. (*E*) Shifts of the molecules indicated by arrows around point defects from their crystallographic positions.

indicate concentrations of the dimers in the surface layer 100–1000 times higher than in the solution bulk (Vekilov et al., submitted for publication).

Interactions between apoferritin monomers

Influence of the sodium acetate buffer concentration

The interactions between apoferritin monomers were characterized by static light scattering experiments with apoferritin monomer solutions, performed in the presence of NaAc buffer. The buffer concentration was varied so that [Na^+] could change between 0.01 and 0.25 M. The respective Debye plots are shown in Fig. 5. The refractive index increment dn/C_p at the salt concentrations used is shown in Table 2. The molecular masses obtained from the intercept of the straight lines through the data with the ordinate axis (see Eq. 12) is ~450 kD for all cases except for 0.2 and 0.25 M NaAc where it is a little higher, ~475 kD. The slope of the lines decreases initially with the addition of electrolyte, but, above ~0.15 M, starts to increase again. These trends are shown in Fig. 6, in terms of a dependence of the dimensionless virial coefficient, B_2, on the concentration of Na^+ ions. The decrease in the repulsion between 0.01 and 0.15 M Na^+ is readily explained in terms of the general DLVO theory: as the concentration of electrolyte increases, the electrostatic repulsion between the molecules is screened (Verwey and Overbeek, 1948; Derjaguin et al., 1987) and the virial coefficient decreases. The further increases in the repulsion (above 0.15 M Na^+), however, cannot be explained in the framework of the DLVO theory, because it always predicts weaker electrostatic repulsion at higher electrolyte concentrations. Hence, we hypothesize that different types of interactions dominate the low and high salt concentration regions. Accordingly, we interpret the experimental results at low and high buffer concentrations separately.

TABLE 2 Refractive index increment dn/dC_p for apoferritin solutions at various salt concentrations.

Salt type and concentration	dn/dC_P (ml/g)
NaAc, 0.01 M	0.259
NaAc, 0.05 M	0.216
NaAc, 0.10 M	0.179
NaAc, 0.15 M	0.160
NaAc, 0.20 M	0.159
NaAc, 0.20 M and $CdSO_4$, 0.01 M	0.162

The low-concentration region is dominated by electrostatics and the respective energy component, $U_{el}(r)$, is (Beresford-Smith et al., 1985)

$$U_{el}(r) = \frac{(z_0 e)^2}{\varepsilon} \frac{\exp(2\kappa a)}{(1 + ka)^2} \frac{\exp(-\kappa r)}{r}. \quad (18)$$

This leads to the following expression for the second osmotic virial coefficient (Petsev and Denkov, 1992)

$$B_2 = 4 + \frac{3(z_0 e)^2}{2\varepsilon kTa} \frac{(1 + 2\kappa a)}{(1 + ka)^2(\kappa a)^2}. \quad (19)$$

In Eq. 19, z_0 is the number of charges per molecule, e is the elementary charge, ε is the dielectric constant of the solvent and κ is the charge-screening parameter (inverse Debye length) defined by

$$\kappa^2 = \frac{4\pi e^2}{\varepsilon kTa} \sum_i n_i z_i^2, \quad (20)$$

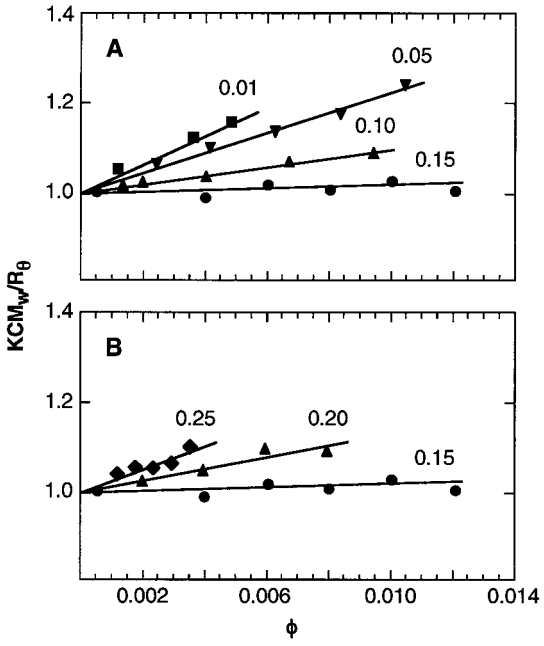

FIGURE 5 Debye plots for apoferritin monomer in NaAc buffer solution. Sodium cation [Na^+] concentrations are indicated in the plots and are in (*A*) between 0.01 and 0.15 M and in (*B*) between 0.15 and 0.25 M.

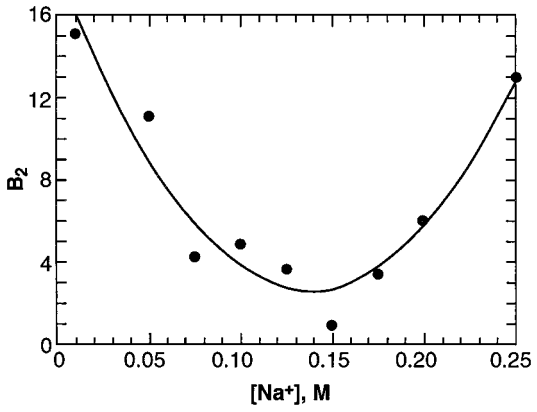

FIGURE 6 Dimensionless second osmotic virial coefficient B_2 for the apoferritin monomer as a function of the sodium cation concentration [Na^+]. Solid line is just a guide for the eye.

where n_i and z_i are number ionic concentration and charge, respectively. The first term in Eq. 19 accounts for the hard sphere interactions of the molecules with a finite size, whereas the second one accounts for the electrostatic repulsion, due to the molecular charge. Eqs. 19 and 20 predict that the second virial coefficient should decrease with increasing electrolyte concentration, and this is what we observe between 0.01 and 0.15 M NaAc. The value of B_2 changes from ~15 to ~4 (lower values could be a manifestation of weak attraction, e.g., of van der Waals origin). This decrease in B_2 in the range 0.01–0.15 M corresponds to the one predicted by Eq. 19 with $z_0 = 24$ (negative). Apoferritin has 624 acidic and 576 basic aminoacid residues on its surface. Dissociation of the acidic groups leads to negative charges, whereas protonation of the basic ones leads to positive charges. Comparing all these numbers cannot result in a strict quantitative conclusion, but clearly shows that $z_0 = 24$ is a reasonable value for pH = 5.0, slightly above the isoelectric point of ~4.0.

The above considerations based on Eq. 19 are only valid in the limiting case when the molecular charge z_0 remains constant with the addition of electrolyte. The other limiting case is when the surface charge varies but the surface potential, Ψ_0, remains constant. Using the simple relationship (valid for low surface charges and potentials) (Beresford-Smith et al., 1985)

$$\Psi_0 = \frac{z_0 e}{\varepsilon a}\frac{1}{(1+\kappa a)}, \tag{21}$$

we obtain the constant potential version of the second osmotic virial coefficient (Petsev and Denkov 1992)

$$B_2 = 4 + \frac{3\Psi_0^2 \varepsilon a}{2kT}\frac{(1+2\kappa a)}{(\kappa a)^2}. \tag{22}$$

Eq. 22 can be fitted to the data in the low electrolyte region (below 0.15 M) using, this time, the surface potential as a free parameter. The value obtained from the fit is $e\Psi_0/kT = 0.54$, or $\Psi_0 = 14.5$ mV. We are not aware of any other experimental data for the surface charges or potentials of apoferritin. The orders of magnitude of our results, however, seem reasonable for protein systems (see e.g., Anderson et al., 1978).

Note that the constant charge and potential cases represent limiting situations and that, in some cases, none of them may be realized. If both the charge and potential vary with increasing electrolyte concentration, a more elaborate model may be required.

As pointed out above, the experimental results at Na^+ concentrations above 0.15 M cannot be explained in terms of electrostatic arguments. We argue that the origin of the high salt repulsion is in the hydration interaction (Petsev and Vekilov, submitted for publication). The nature of these interactions has not been uniquely identified yet. Hence, there is no straightforward expression relating the hydration force to the salt concentration, and we are unable to perform analysis similar to that in the electrostatic case. We restrict ourselves to approximate estimations that show that our observations are compatible with other empirical observation of this type of forces in the literature. According to a formula, derived by fitting surface force experimental data, the hydration energy U_{hyd} depends on the distance from the molecular center r as (Pashley, 1982; Israelachvili, 1991; Somasundaran et al., 1997)

$$U_{hyd}(r) = \pi a L f_0 \exp\left[\frac{-(r-2a)}{L}\right]. \tag{23}$$

Here, f_0 and L are empirically determined surface energy density and decay length. Surface force measurements (Pashley, 1982; Israelachvili, 1991) have yielded results for $f_0 \approx 3$–30 mJ/m and $L \approx 0.6$–1.1 nm. The limits for the decay length, L, could be even wider (Trokhymchuk et al., 1999). To test the feasibility of our data, we choose decay length $L = 2 \times 0.72$ nm = 1.44 nm, i.e., twice the diameter of the hydrated sodium ion (Israelachvili, 1991). This corresponds to each apoferritin molecule having a layer of hydrated sodium ions in its immediate vicinity. Because apoferritin bears a negative charge at pH = 5.0, Na^+ are the counterions that accumulate in the vicinity of the molecular surface. Introducing Eq. 23 into Eq. 14, and also taking into account the hard sphere contribution, we obtain $B_2 \approx 13$ for 0.25 M NaAc. This corresponds to $f_0 = 12.5$ mJ/m, which is in the middle of the empirical range for this parameter (Pashley, 1982; Israelachvili, 1991).

The repulsion between the apoferritin molecules at high ionic strengths suggests that small ions are an important factor for protein stability. This is in accordance with other experimental (Israelachvili, 1991; Molina-Bolivar et al., 1996, 1997, 1998; Molina-Bolivar, 1999; Molina-Bolivar and Ortega-Vinuesa, 1999; Pashley, 1981a,b, 1982; Pashley and Israelachvili, 1984) and theoretical (Paunov et al., 1996; Paunov and Binks, 1999; Trokhymchuk et al., 1999) studies of hydration interactions. An appropriate example are the kinetic studies of protein-stabilized latex particles. They show that, for negatively charged protein-covered particles in the presence of NaCl, there exists a hydration repulsion that disappears when the charge is converted to positive (Molina-Bolivar et al., 1996, 1997, 1998; Molina-Bolivar, 1999; Molina-Bolivar and Ortega-Vinuesa, 1999). In other words, Na^+ ions induce hydration repulsion, whereas $C1^-$ ions do not. This fact can be related to the greater hydration affinity of Na^+ compared to $C1^-$ (Marcus, 1988; Israelachvili, 1991). Furthermore, note that studies of the interactions between lysozyme molecules in an NaAc buffer (Muschol and Rosenberger, 1995) show no evidence for increased repulsion at high ionic strengths. However, in contrast to apoferritin, at pH ~5, lysozyme has a positive charge, Na^+ are co-ions and are expelled from the vicinity of the protein surface.

From a colloidal viewpoint, proteins are weakly charged particles, whereas the physiological ionic strength at 0.15 M is relatively high. This means that electrostatic stabilization is hardly the most likely candidate to explain protein stability in living organisms. Hydration repulsion is a better option, and its sensitivity toward the nature of the particular ions allows for precise regulation of their biological functions. A very important example is related to hemoglobin S, mutant human hemoglobin whose aggregation in the red blood cells causes sickle cell anemia. The solubility of this protein increases with the increase of the concentration of Na or K monovalent salts from 0 to 0.3 M, i.e., immediately below and above the physiological ionic strength (Eaton and Hofrichter, 1990). This indicates increase in the intermolecular repulsion (George and Wilson, 1994; Rosenbaum and Zukoski, 1996; Velev et al., 1998) with higher ionic strength, similar to the apoferritin behavior attributed above to hydration forces.

Influence of $CdSO_4$

Apoferritin crystallizes readily when $CdSO_4$ is added to the solution (Lawson et al., 1991; Hempstead et al., 1997; Thomas et al., 1998). X-ray crystallography has shown that Cd^{2+} partake in covalent bonds between the protein molecules (Lawson et al., 1991). To characterize the effects of the Cd^{2+} ions on the intermolecular interactions in the solution, we performed DLS determinations of the molecular size distributions and SLS determinations of the protein molecular mass and the second osmotic virial coefficients of apoferritin monomers in the presence of NaAc buffer and $CdSO_4$. The used buffer concentrations were 0.10, 0.15, and 0.20 M, whereas the concentration of $CdSO_4$ was 0.2% (w/w) or ~0.01 M (~10 times lower than typically used in crystallization) in all experiments. The size distribution in Fig. 7 indicates a monodisperse sample with an average hydrodynamic diameter of ~13.5 nm. This is slightly higher than the result for the apoferritin monomer in the absence of Cd^{2+} in Table 1. The respective molecular masses, determined by SLS, are between 560 and 580 kD, also higher than in the absence of Cd^{2+}, indicating weak aggregation of the monomer. This should not affect the relevance of the results for the dimensionless virial coefficients. As evidenced by Eq. 16, the slight increase of the molecular mass and radius are taken into account explicitly. The values for B_2 in the presence of 0.01 M $CdSO_4$ extracted from the straight lines in Fig. 8 are: −3.01 for 0.10 M buffer concentration, −0.406 for 0.15 M, and −0.985 for 0.20 M. Because all values for the dimensionless virial coefficient below 4 (hard sphere) indicate attraction, we can conclude that the addition of 0.01 M $CdSO_4$ is sufficient to overcome the repulsion induced by the available concentration of Na^+. This is a rather remarkable result: the Na^+ and Cd^{2+} ions have similar hydration ability; their average coordination numbers for water molecules are ~6 and ~5.2, respectively (Marcus, 1988). Apparently, the covalent intermolecular binding, mediated by the Cd^{2+} ions, overpowers any other effects that the two counterions may have.

Interactions between dimer molecules in Na^+- and Cd^{2+}-containing solutions

As-received apoferritin and solution contain about 50% of the dry protein mass of dimers and higher oligomers (Thomas et al., 1998). These commercial preparations represent solutions in 0.1 M NaCl or NaAc. Because we found, see above, strong repulsion between the monomer molecules at Na^+ concentrations that straddle those in the as-received solution, a legitimate question is why are there any dimers present in the solution at all? To elucidate this issue, we studied by static light scattering the molecular interactions in dimer solutions at 0.2 M Na^+, at which concentration the repulsive forces between the monomers are even stronger than at 0.1 M Na^+. The Debye plot in Fig. 9 indicates that, contrary to the monomers in Figs. 5 *B* and 6, the dimers do

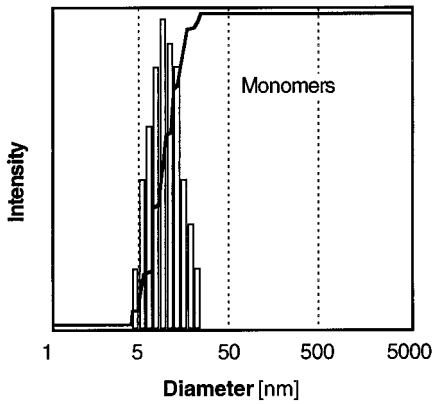

FIGURE 7 CONTIN results for the size distribution of apoferritin monomers in the presence of 0.01 M $CdSO_4$: (*A*) buffer concentration 0.10 M, (*B*) buffer concentration 0.15 M, and (*C*) buffer concentration 0.20 M.

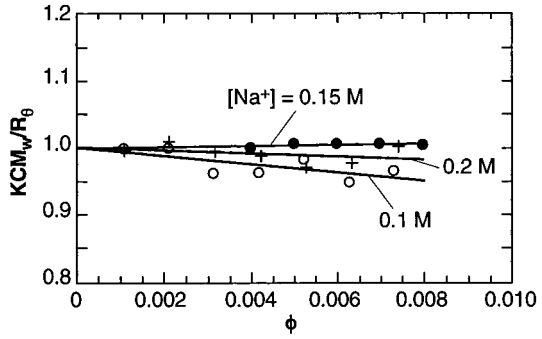

FIGURE 8 Debye plots for apoferritin monomer in NaAc buffer solution in the presence of 0.01 M Cd^{2+}. Sodium cation [Na^+] concentrations are indicated in the plots. Note that, in the presence of Cd^{2+}, there is no correlation between [Na^+] and the slope of the Debye plots.

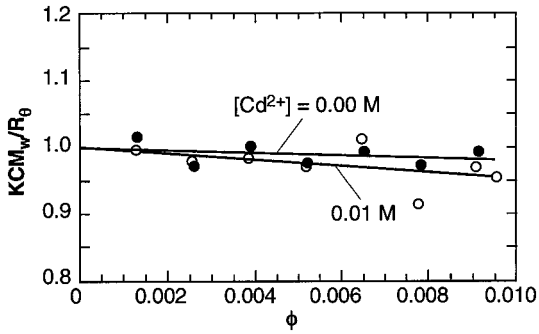

FIGURE 9 Debye plots for apoferritin dimer in the presence of 0.2 M Na^+, the $[Na^+]$ at which crystallization occurs. Cadmium cation concentration $[Cd^{2+}]$ is indicated in the plots.

not repel but rather attract. These observations support the hypothesis, discussed above in relation to the dimer structure and their incorporation into the crystals as defect-causing impurities in Fig. 4, that the dimer formation is caused by the partial denaturation of the monomer. This denaturation exposes groups that locally decrease the repulsion and increase the attraction between them, such as hydrophobic groups that are tucked inside the native protein. The formation of the dimer does not saturate all possible hydrophobic patches on the molecular surface, and this leads to attraction even between the dimers.

The addition of Cd^{2+} increases the attraction between the dimer molecules even further, see Debye second plot in Fig. 9. The slope of the straight line, i.e., the second osmotic virial coefficient, is similar to that for the monomer under identical conditions in Fig. 8. On the basis of this similarity, one would expect the dimer to compete with the monomer for adsorption on the crystal surface and incorporation into the crystal. This corresponds to the actual observations in Fig. 4.

CONCLUSIONS

The overall interactions between the monomer apoferritin molecules in NaAc are repulsive with a minimum around $[Na^+]$ of 0.10–0.15 M. Below these values, the second osmotic virial coefficient decreases with the increasing buffer concentration in conformity to the charge-screening concept of the DLVO theory of colloid stability. Above 0.15 M, however, the virial coefficient increases with the buffer concentration, which is beyond the predictions of this theory. We argue that this repulsion is due to hydration interaction, related to counterion-assisted structuring of the water in the vicinity of the protein molecules. The addition of $CdSO_4$, a crystallization-inducing agent, has a powerful effect on the system, overwhelming the repulsion and shifting the virial coefficient values into the attractive range below four.

The diffusion coefficient of the dimers, the most common impurity in apoferritin solutions, agrees with estimates for a prolate spheroid shape. This shape is confirmed by a direct AFM observation.

The formation of dimers and higher aggregates in the commercial product occurs in the absence of $CdSO_4$ and is surprising, considering the overall repulsion between the monomers. We present evidence suggesting that this type of oligomerization may be induced by partial denaturation of the apoferritin monomers that expose hydrophobic parts of the molecule to the water environment and make oligomerization a favored option. When a dimer adsorbs on a crystal surface and is then trapped into the growing crystal, it displaces three, rather then two, monomer molecules. This suggests that the binding sites within the dimer differ from the Cd^{2+} mediated bonds in the crystal lattice and the arrangement of the monomers in the dimer is different from that of a pair of monomers in the crystals.

In solutions containing dimers only, the molecular interactions are attractive even in the absence of Cd^{2+}, and the addition of Cd^{2+} only makes these interactions more attractive. The strong attraction even in the absence of Cd^{2+} may be another effect of the partial denaturation of the constituent monomers. As a consequence, the dimers exhibit a higher propensity for aggregation and other transitions to a solid state than the monomers. These observations and considerations likely underlie the preferential adsorption of the dimers on the surface of the growing crystal, leading to a concentration of the dimers in the surface layer 100–1000 times higher than in the solution bulk.

We thank L. Carver for expert graphics preparation.

This work was supported by National Institutes of Health grant NIH R01 HL58038 and National Aeronautics and Space Administration grants NAG8-1354 and 97 HEDS-02-50).

REFERENCES

Anderson, J. L., F. Rauh, and A. Morales. 1978. Particle diffusion as a function of concentration and ionic strength. *J. Phys. Chem.* 82: 608–615.

Basu, S., and M. M. Sharma. 1994. Effect of dielectric saturation on disjoining pressure in thin films of aqueous electrolyte. *J. Colloid Interface Sci.* 165:355–366.

Beresford-Smith, B., D. Y. C. Chan, and D. J. Mitchell. 1985. The electrostatic interaction in colloidal systems with low added electrolyte. *J. Colloid Interface Sci.* 105:216–234.

Besseling, N. A. M. 1997. Theory of hydration forces between surfaces. *Langmuir.* 13:2113–2122.

Brenner, H. 1974. Rheology of a dilute suspension of axisymmetric Brownian particles. *Int. J. Multiphase Flow* 1:195–341.

Derjaguin, B. V., N. V. Churaev, and V. M. Muller. 1987. *Surface Forces.* Plenum, New York.

Eaton, W. A., and J. Hofrichter. 1990. Sickle cell hemoglobin polymerization. *In* Advances in Protein Chemistry. C. B. Anfisen, J. T. Edsall, F. M. Richards, and D. S. Eisenberg, editors. Vol. 40. Academic Press, New York 63–279.

Forsman, J., C. E. Woodward, and B. Jonsson. 1997. The origins of hydration forces: Monte Carlo simulations and density functional theory. *Langmuir.* 13:5459–5464.

George, A., and W. W. Wilson. 1994. Predicting protein crystallization from dilute solution property. *Acta Cryst. D.* 50:361–365.

Hempstead, P. D., S. J. Yewdall, A. R. Fernie, D. M. Lawson, P. J. Artymiuk, D. W. Rice, G. C. Ford, and P. Harrison. 1997. Comparison of the three-dimensional structure of recombinant human H and horse L ferritins at high resolution. *J. Mol. Biol.* 288:424–448.

Henderson, D., and M. Lozada-Cassou. 1986. A simple theory for the forces between spheres immersed in a fluid. *J. Colloid Interface Sci.* 114:180–183.

Henderson, D., and M. Lozada-Cassou. 1994. Does dielectric saturation provide a plausible explanation of the hydration solvation force? *J. Colloid Interface Sci.* 162:508–509.

Israelachvili, J. N. 1991. Intermolecular and Surface Forces. Academic, New York.

Israelachvili, J. N., and H. Wennerstrom. 1996. Role of hydration and water structure in biological and colloidal interactions. *Nature.* 379: 219–225.

Lawson, D. M., P. J. Artymiuk, et al. 1991. Solving the structure of human H ferritin by genetically engineered intermolecular crystal contacts. *Nature.* 349:541–544.

Marcelja, S., and N. Radic. 1976. Repulsion of interfaces due to boundary water. *Chem. Phys. Lett.* 42:129–130.

Marcus, Y. 1988. Ionic radii in aqueous solutions. *Chem. Rev.* 88: 1475–1498.

McQuarrie, D. A. 1973. Statistical Mechanics. Harper & Row, New York. 328–335.

Molina-Bolivar, J. A., F. Galisteo-Gonzalez, and R. Hidalgo-Alvares. 1999. Colloidal aggregation in energy minima of restricted depth. *J. Chem. Phys.* 110:5412–5420.

Molina-Bolivar, J. A., F. Galisteo-Gonzalez, and R. Hidalgo-Alvares. 1996. Stabilization of protein–latex complexes at high ionic strength. *Colloids Surf. B.* 8:73–80.

Molina-Bolivar, J. A., F. Galisteo-Gonzalez, and R. Hidalgo-Alvares. 1997. Colloidal stability of protein–polymer systems: a possible explanation by hydration forces. *Phys. Rev. E.* 55:4522–4530.

Molina-Bolivar, J. A., F. Galisteo-Gonzalez, and R. Hidalgo-Alvares. 1998. Cluster morphology of protein-coated polymer colloids. *J. Colloid Interface Sci.* 208:445–454.

Molina-Bolivar, J. A., and J. L. Ortega-Vinuesa. 1999. How proteins stabilize colloidal particles by means of hydration forces. *Langmuir.* 15:2644–2653.

Muschol, M., and F. Rosenberger. 1995. Interactions in undersaturated and supersaturated lysozyme solutions: static and dynamic light scattering results. *J. Chem. Phys.* 103:10424–10432.

Pashley, R. M. 1981a. DLVO and hydration forces between mica surfaces in Li+, Na+, K+ and Cs+ electrolyte solutions: a correlation of double-layer and hydration forces with surface cation exchange properties. *J. Colloid Interface Sci.* 83:531–546.

Pashley, R. M. 1981b. Hydration forces between mica surfaces in aqueous electrolyte solutions. *J. Colloid Interface Sci.* 80:153–162.

Pashley, R. M. 1982. Hydration forces between mica surfaces in electrolyte solutions. *Adv. Colloid Interface Sci.* 16:57–62.

Pashley, R. M., and J. N. Israelachvili. 1984. DLVO and hydration forces between mica surfaces in Mg2+, Ca2+, Sr2+ and Ba2+ chloride solutions. *J. Colloid Interface Sci.* 97:446–455.

Paunov, V. N., and B. P. Binks. 1999. Analytical expression for the electrostatic disjoining pressure taking into account the excluded volume of the hydrated ions between charged interfaces in electrolyte. *Langmuir.* 15:2015–2021.

Paunov, V. N., R. I. Dimova, P. A. Kralchevsky, G. Broze, and A. Mehreteab. 1996. The hydration repulsion between charged surfaces as an interplay of volume exclusion and dielectric saturation effects. *J. Colloid Interface Sci.* 182:239–248.

Petsev, D. N., and N. D. Denkov. 1992. Diffusion of charged colloidal particles at low volume fraction: theoretical model and light scattering experiments. *J. Colloid Interface Sci.* 329:329–344.

Provencher, S. W. 1979. Inverse problems in polymer characterization; direct analysis of polydispersity with photon correlation spectroscopy. *Makromol. Chem.* 180:201–209.

Provencher, S. W. 1982a. A constrained regularization method for inverting data represented by linear algebraic equations. *Comp. Phys. Com.* 27:213–227.

Provencher, S. W. 1982b. CONTIN: a general purpose constrained regularization program for inverting noisy linear algebraic and integral equations. *Comp. Phys. Com.* 27:229–242.

Pusey, P. N., and R. J. A. Tough. 1985. Particle interactions. *In* Dynamic Light Scattering. R. Pecora, editor. Plenum Press; New York. 85–179.

Rosenbaum, D. F., and C. F. Zukoski. 1996. Protein interactions and crystallization. *J. Cryst. Growth.* 169:752–758.

Schmitz, K. S. 1990. Dynamic Light Scattering by Macromolecules. Academic Press, New York.

Somasundaran, P. B., B. Markovic, S. Krishnakumar, and X. Yu. 1997. Colloid systems and interfaces—stability of dispersions through polymer and surfactant adsorption. *In* Handbook of Surface and Colloid Science. K. Birdi, editor. CRC Press, New York.

Thomas, B. R., D. Carter, and F. Rosenberger. 1998. Effect of microheterogenity on horse spleen apoferritin crystallization. *J. Crystal Growth.* 187:499–510.

Thomas, B. R., P. G. Vekilov, and F. Rosenberger. 1996. Heterogenity determination and purification of commercial hen egg-white lysozyme. *Acta Cryst. D.* 52:776–784.

Trokhymchuk, A., D. Henderson, and D. T. Wasan. 1999. A molecular theory of the hydration force in an electrolyte solution. *J. Colloid Interface Sci.* 210:320–331.

Velev, O., E. W. Kaler, and A. M. Lenhoff. 1998. Protein interactions in solution characterized by light and neutron scattering: comparison of lysozyme and chymotrypsinogen. *Biophys. J.* 75:2682–2697.

Verwey, E. J., and J. T. G. Overbeek. 1948. Theory and Stability of Lyophobic Colloids. Elsevier, Amsterdam.

Zimm, B. H. 1948. The scattering of light and the radial distribution function of high polymer solutions. *J. Chem. Phys.* 6:1093–1099.